Inorganic Chemistry

Article

pubs.acs.org/IC

Intermolecular Interactions in Solid-State Metalloporphyrins and Their Impacts on Crystal and Molecular Structures

Seth C. Hunter,[†] Brenda A. Smith,[†] Christina M. Hoffmann,*[,‡] Xiaoping Wang,*[,‡] Yu-Sheng Chen,[§] Garry J. McIntyre,[∥,⊥] and Zi-Ling Xue*[,†]

[†]Department of Chemistry, The University of Tennessee, Knoxville, Tennessee 37996, United States

[‡]Chemical and Engineering Materials Division, Oak Ridge National Laboratory, Oak Ridge, Tennessee 37830, United States

[§]ChemMatCARS, Center for Advanced Radiation Sources, The University of Chicago, Argonne, Illinois 60439, United States

[∥]Institut Laue-Langevin, BP 156, 38042 Grenoble Cedex 9, France

Supporting Information

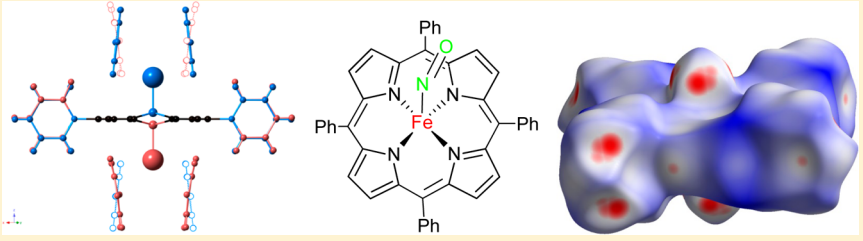

ABSTRACT: A variable-temperature (VT) crystal structure study of [Fe(TPP)Cl] (TPP^{2-} = *meso*-tetraphenylporphyrinate) and Hirshfeld surface analyses of its structures and previously reported structures of [M(TPP)(NO)] (M = Fe, Co) reveal that intermolecular interactions are a significant factor in structure disorder in the three metalloporphyrins and phase changes in the nitrosyl complexes. These interactions cause, for example, an 8-fold disorder in the crystal structures of [M(TPP)(NO)] at room temperature that obscures the M−NO binding. Hirshfeld analyses of the structure of [Co(TPP)(NO)] indicate that the phase change from $I4/m$ to $P\bar{1}$ leads to an increase in void-volume percentage, permitting additional structural compression through tilting of the phenyl rings to offset the close-packing interactions at the interlayer positions in the crystal structures with temperature decrease. X-ray and neutron structure studies of [Fe(TPP)Cl] at 293, 143, and 20 K reveal a tilting of the phenyl groups away from being perpendicular to the porphyrin ring as a result of intermolecular interactions. Structural similarities and differences among the three complexes are identified and described by Hirshfeld surface and void-volume calculations.

INTRODUCTION

A key structural feature of the O_2-free hemes in hemoglobin and myoglobin is that the active center contains a five-coordinate Fe porphyrin. In both proteins, O_2 binds to the iron atom, turning the five-coordinate heme into a six-coordinate complex. Five-coordinate Fe porphyrin systems[1−3] such as [Fe(TPP)Cl] (Figure 1) have thus been actively studied to provide insight into the physical and chemical properties of the hemes.[4−10] The first reported structure of [Fe(TPP)Cl] was incorrectly solved as [Fe(TPP)(OH)]·H_2O in the $I4$ space group.[4a] This structure was reanalyzed by Hoard et al. in the higher symmetry $I4/m$ space group as [Fe(TPP)Cl].[4b] Monoclinic [Fe(TPP)Cl] crystals in the $P2_1/n$ space group were obtained by Scheidt et al. through decomposition of [Fe(TPP)(NO)] in a CH_2Cl_2 solution containing nitrate and nitrite ions.[9] A structure of [Fe(TPP)Cl] at 100 K, in the $I4/m$ space group, was solved by Scheidt and co-workers.[11] Most recently [Fe(TPP)Cl] at 293 K was refined in the $I4$ space group by Hadjikakou et al. with two superimposed independent molecules having different distances of the Fe atom to the plane defined by the four N atoms of the porphyrin.[12]

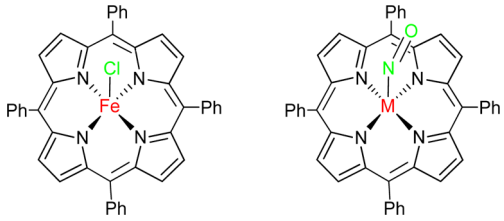

Figure 1. [Fe(TPP)Cl] and [M(TPP)(NO)] (M = Fe, Co).

Nitric oxide (NO) is a vital cellular signaling agent in many physiological and pathological processes.[13] Its coordination to heme proteins is involved in several fundamental processes such as neuronal communication,[14] muscle relaxation,[15] platelet deaggregation,[16] and myocardial function.[17] Five-coordinate Fe−NO porphyrins are active complexes in the signaling events. The nitrosyl metalloporphyrins [M(TPP)(NO)] (M = Fe, Co) were first synthesized and characterized by Scheidt et al. about 40 years ago.[18] These two complexes, displaying tilted

Received: July 3, 2014
Published: October 23, 2014

   dx.doi.org/10.1021/ic5015835 | *Inorg. Chem.* 2014, 53, 11552−11562

Table 1. Crystal Data and Structural Refinement Details for [Fe(TPP)Cl][a,b]

space group	*I*4	*I*4	*I*4	*I*4
temp (K)	293(2)	143(2)	20(2)	20(2)
a (Å)	13.5374(2)	13.504(3)	13.4830(5)	13.4761(6)
c (Å)	9.8247(2)	9.731(10)	9.6849(6)	9.6889(6)
V (Å^3)	1800.49(5)	1774.5(19)	1760.63(14)	1759.56(16)
Z	2	2	2	2
radiation type	Mo Kα	Mo Kα	synchrotron	neutron
wavelength (Å)	0.71073	0.71073	0.41328	0.8387(2)
μ (mm^{-1})	0.530	0.538	0.288	0.112
cryst size (mm^3)	0.70 × 0.20 × 0.10	0.50 × 0.20 × 0.10	0.04 × 0.04 × 0.04	1.50 × 1.00 × 1.00
no. of measd, unique, obsd ($I > 2\sigma(I)$) rflns	9622, 2120, 2015	7973, 2002, 1772	36372, 11751, 10231	1893, 1263, 1045
R_{int}	0.0165	0.0536	0.0488	0.0286
R ($F^2 > 2\sigma(F^2)$), $R_w(F^2)$, S	0.0318, 0.0885, 1.059	0.0481, 0.1487, 1.062	0.0352, 0.1092, 1.004	0.0399, 0.0757, 1.137
no. of rflns	2120	2002	11751	1263
no. of params	119	120	136	194
no. of restraints	1	1	18	52
$\Delta\rho_{max}$, $\Delta\rho_{min}$ (e Å^{-3} or fm Å^{-3})	0.213, −0.261	0.427, −0.316	0.707, −0.512	0.543, −1.114
Fe−Cl occupancy: minor, major	0.363(1), 0.637(1)	0.367(2), 0.633(2)	0.4084(5), 0.5916(5)	0.39(2), 0.61(2)

[a][Fe(TPP)Cl]: chemical formula, $FeN_4C_{44}H_{28}Cl$; M_r = 704.00; crystal system, tetragonal. For the structures at 293 and 143 K refined in *I*4/*m*, crystal data and refinement details and a comparison with those in *I*4 are given in Table S1 (Supporting Information). [b]Computer programs: Bruker APEX2, Bruker SAINT and SHELXL97,[27] Bruker SHELXTL.

M−NO binding, provided the initial insight into the coordination chemistry of nitric oxide to metalloporphyrins. However, both complexes crystallize in the tetragonal *I*4/*m* space group with 8-fold disorder of the O atom in the NO ligand at room temperature, significantly obscuring the binding of NO to Fe or Co atoms and the structural features of the complexes.[11,13g,18] Electronic and vibrational properties of the complexes and their structures, including the tilted binding and dynamics of the NO ligands on the complexes, have also been studied.[13d,19] Recently, the structures have been investigated by VT X-ray diffraction[11,13g] and DFT calculations.[19a] Both species were found to undergo a lowering of the space group symmetry from tetragonal *I*4/*m* to the triclinic $P\bar{1}$, upon lowering of the temperature. From bond length and angle analysis no clear benefit could be identified, and it is thus not obvious why the phase changes occur.[11,13g]

We have studied VT X-ray and neutron structures of [Fe(TPP)Cl] and used Hirshfeld surface analysis for the crystal structures of [Fe(TPP)Cl] and [M(TPP)(NO)] (M = Fe, Co). We chose these two nitrosyl compounds for comparison with [Fe(TPP)Cl], where the symmetric Cl can be juxtaposed to the asymmetric NO ligand and iron can be contrasted with cobalt as the central atom. The Hirshfeld surface analysis, recently developed by Spackman and co-workers, allows for the comparison of molecular structures by examining interactions of an individual molecule with its nearest neighbor molecules while maintaining a whole-of-molecule approach.[20−22] A Hirshfeld surface is an isosurface calculated from the weight function $w(\mathbf{r})$ of the sum of spherical atom electron densities (eq 1), where $\rho_{promolecule}(\mathbf{r})$ is the sum of the molecular electron density over the atoms in the molecule of interest (the promolecule) and $\rho_{procrystal}(\mathbf{r})$ is the similar sum over the crystal (the procrystal).[20−22]

$$w(\mathbf{r}) = \frac{\rho_{promolecule}(\mathbf{r})}{\rho_{procrystal}(\mathbf{r})} = \sum_{A\in molecule} \rho_A(\mathbf{r}) / \sum_{A\in crystal} \rho_A(\mathbf{r}) \quad (1)$$

The isosurface separates a molecule (promolecule) from its nearest neighbors (procrystal) at a given density level. From the Hirshfeld surface, distances to the nearest atoms outside (external), d_e, and inside (internal), d_i, are readily defined, and the surface gives a visual 3-D representation of the intermolecular close contacts in the crystal. Using the d_e, d_i pairs, the Hirshfeld surface can be reduced to a 2-D histogram, giving a unique fingerprint plot for molecular interactions in the crystal.[21,22] Void volumes in the crystal can be readily determined using the same isosurfaces of electron density, by looking at areas in the crystal where the electron density is the lowest.[23] Other earlier methods, in comparison, rely on the approximation of a molecule as a set of fused spheres with van der Waals radii and are thus limited in scope.[20−23] Hirshfeld surface analysis has been used to explore permanent voids, cavities, and channels in porous materials such as MOFs (metal−organic frameworks) and COFs (covalent organic frameworks).[23] Hirshfeld surface analysis is an excellent tool to compare compounds with respect to their molecular environment and interactions independent of the overall space group symmetry. The Hirshfeld surface and void volume analyses of the crystal structures of [Fe(TPP)Cl] and [M(TPP)(NO)] (M = Co, Fe) in the current work provide an understanding of their crystal and molecular structures at room and lower temperatures and, more importantly, the phase changes in [M(TPP)(NO)]. These analyses show that intermolecular interactions lead to the observed disorders at room temperature in [M(TPP)(NO)] and their phase changes at lower temperatures, affecting both their structures and the dynamics of the NO ligand rotation. Without the use of Hirshfeld analyses, it is difficult to describe the structure changes in the nitrosyl complexes in a comprehensive manner, as the phase changes involve different space groups (*I*4/*m* → $P\bar{1}$).[11,13g]

EXPERIMENTAL SECTION

Synthesis.[24] [Fe(TPP)Cl], purchased from Strem Chemicals, and solvents (Analytical Reagents) were used without further purification. [Fe(TPP)Cl] was also prepared by modified published procedures.[4b] Wet chloroform was prepared by adding water to chloroform (Certified ACS), and the mixture was shaken and then allowed to settle. Wet chloroform at the bottom was then removed for the use below.

dx.doi.org/10.1021/ic5015835 | Inorg. Chem. 2014, 53, 11552−11562

[Fe(TPP)Cl] (0.05 mmol) was dissolved in wet chloroform (4 mL) and layered with a 1/3 wet chloroform/absolute ethanol mixture (4 mL). The sample container was sealed with Parafilm. After the layers had completely diffused together—in ca. 5−7 days—the solution was allowed to evaporate very slowly for an additional ca. 7 days. Crystals of sizes up to 1 × 2 × 2 mm^3 were observed and collected. A photograph of the crystal used in the neutron diffraction study is given in Figure S1 (Supporting Information). This procedure gave consistently disordered crystals with a slight asymmetric occupancy (ca. 0.40/0.60) of the Fe−Cl part, as discussed below.

Diffraction Data Collection. X-ray diffraction data at 293(2) and 143(2) K were collected on a Bruker AXS Smart 1000 X-ray diffractometer equipped with a CCD area detector and a graphite-monochromated Mo source (Kα radiation, 0.71073 Å) and fitted with an upgraded Nicolet LT-2 low-temperature device (SMART APEX II systems; Precision Cryogenic Systems Inc.). A suitable crystal of size 0.50 × 0.20 × 0.10 mm^3 was coated with Paratone-N oil (Exxon Chemical Americas, Houston, TX, USA) and mounted on a glass fiber.

The lowest temperature synchrotron X-ray diffraction data were collected on another crystal at 20(2) K on a Bruker D8 diffractometer on the ChemMatCARS beamline at the Advanced Photon Source/Argonne National Laboratory (APS/ANL).[25] The diffractometer is equipped with a Bruker 6000 CCD detector. The crystal was coated with Paratone-N oil (Exxon), mounted on a glass fiber, and measured under a stream of helium at 20(2) K.

Global refinements for the unit cell and data reduction were performed with the SAINT program for the X-ray diffraction data collected at 293(2) and 143(2) K.[26] Cell refinement and data reduction for the X-ray data at 20(2) K were carried out using the APEX2 program package.[27] Empirical absorption correction was performed with SADABS.[28] The space group for structure solution and refinement was determined from systematic absences using XPREP.[26]

Neutron diffraction data of [Fe(TPP)Cl] were collected at 20(0.2) K on a 1.5 × 1.0 × 1.0 mm^3 tetragonal-bipyramidal crystal (Figure S1, Supporting Information) on the four-circle diffractometer D9 at the Institut Laue-Langevin, Grenoble, France, in a beam of wavelength 0.8387(2) Å obtained by reflection from a Cu(220) monochromator. D9 is equipped with a small two-dimensional area detector, whose main advantage for this measurement was to allow optimal delineation of the peak from the considerable background due to the large proportion of H atoms in this sample.[29] To avoid strain while cooling, the crystal was wrapped in Al foil before being glued to a V pin and mounted in a closed-cycle He refrigerator. Two equivalents of most unique reflections to 0.68 $Å^{-1}$ in sin θ/λ were collected at 20(0.2) K. For all data, background corrections following the method of Wilkinson et al.[30] as well as Lorentz corrections were applied. Absorption corrections were made by Gaussian integration using the calculated attenuation coefficient μ = 0.112 mm^{-1}, with account taken of the absorption for hydrogen atoms[31,32] with transmission range 0.852−0.891. A total of 1901 independent reflections were collected.[31,32]

Structure Determination. X-ray structures of [Fe(TPP)Cl] at 293, 143, and 20 K were solved by direct methods using SHELXS and refined using the SHELXTL proprietary software package.[33] The neutron structure at 20 K was refined using SHELX97.[33] Non-H atoms in all data and the H atoms in the neutron data were refined with anisotropic displacement parameters. C and H atoms in the disordered phenyl ring were refined with distance constraints. For the X-ray data, H atoms were placed at calculated positions, with isotropic displacement parameters constrained to the equivalent isotropic displacement parameters of the connected C atoms (U_{iso}(H) = 1.2[U_{eq}(C)]). The structures were checked using PLATON.[34] Crystal data and structural refinement details are given in Table 1. Bond lengths and angles are given in Table S2 (Supporting Information).

Hirshfeld Surface Calculations. Hirshfeld surfaces, fingerprint plots, and void volumes were calculated using CrystalExplorer (version 3.1) software from the crystal structure coordinates supplied as CIF files.[35] The X-ray CIF files of [Fe(TPP)Cl] from the current work and in the literature were used.[9a,11,12] For [Fe(TPP)(NO)] and [Co(TPP)(NO)], the published CIFs were used.[13g,11] Hirshfeld surfaces were calculated at an isovalue of 0.5 e au^{-3}. Void volumes were calculated using an isovalue of 0.002 e au^{-3}.[23]

RESULTS AND DISCUSSION

Crystal and Molecular Structures of [Fe(TPP)Cl] at 293, 143, and 20 K.[24] For a detailed structure comparison, it is important to look at the specific point group symmetry of the molecules with respect to the overall structure symmetry. The Fe(III) ion in the [Fe(TPP)Cl] molecule is five-coordinated with apical Cl and four N of the planar porphyrin ligand on the mirror plane perpendicular to the *c* axis. Due to the asymmetric coordination, the Fe atom moves about 0.39 Å out of the porphyrin plane toward the Cl atom to give an idealized C_{4v} point-group symmetry. The porphyrin plane holds four phenyl rings at 90° to the plane. For the crystal structure reported in the *I*4/*m* space group,[4b] the origin (0,0,0) is at the center of the planar porphyrin with overall idealized C_{4h} point-group symmetry. The crystal site symmetry at the origin is higher than the C_{4v} symmetry for a single ordered [Fe(TPP)Cl] molecule. The apparent higher site symmetry imposes a 50/50 disorder of the axial Fe−Cl part above and below the porphyrin

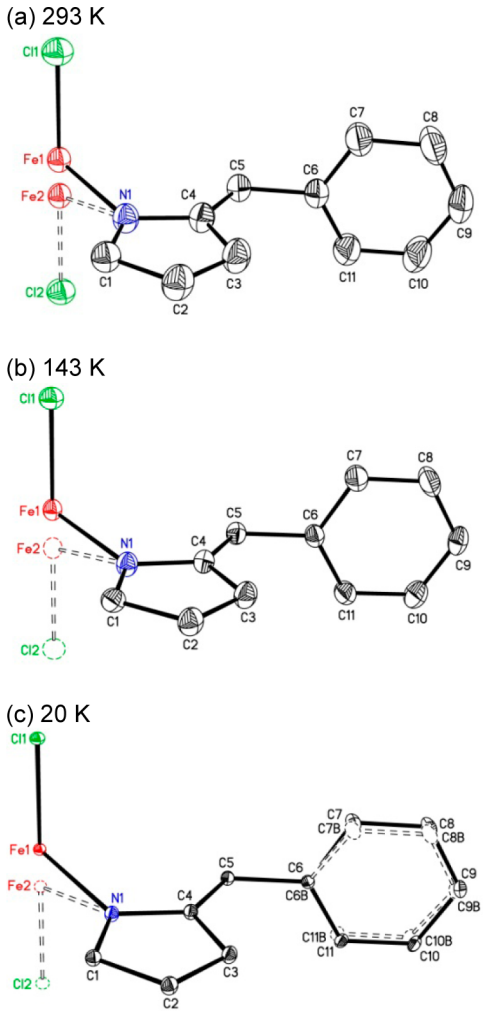

Figure 2. ORTEP drawings of the asymmetric unit of [Fe(TPP)Cl] in *I*4 from X-ray diffraction data. Thermal ellipsoids are drawn at the 30% probability level. H atoms are omitted for clarity. Disordered atoms are drawn as dashed lines.

dx.doi.org/10.1021/ic5015835 | Inorg. Chem. 2014, 53, 11552−11562

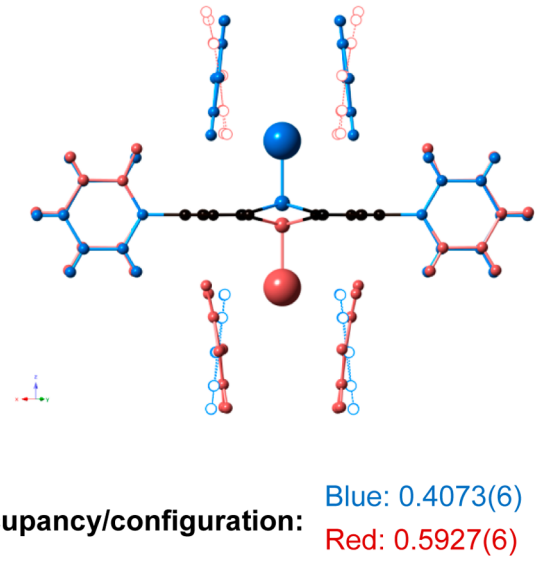

Figure 3. Plot of the disorder in phenyl groups of [Fe(TPP)Cl] at 20 K (X-ray). Filled and empty spheres represent the associated and opposing phenyl rings, respectively.

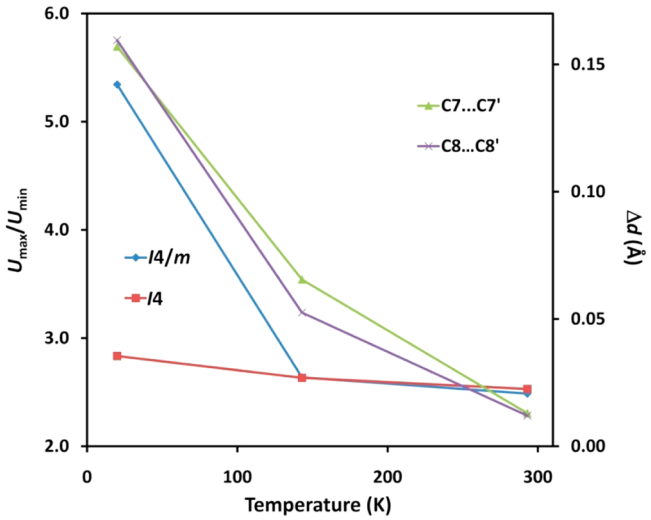

Figure 4. Graph showing changes, with temperature, of the thermal ellipsoid distortion ratio (U_{max}/U_{min}) in $I4/m$ and $I4$ (left axis) and the C7−C7′ and C8−C8′ distances of the phenyl ring (right axis).

plane in the $I4/m$ structure. Since the porphyrin ring of the TPP^{2-} ligand is rigid and prefers planar symmetry with all atoms located on the mirror plane,[36] it leaves only two C (and the associated H) atoms of the connected phenyl rings on the general positions above and below the mirror plane to respond freely to physical restraints imposed by decreasing temperature and rotate with respect to the porphyrin plane.

The [Fe(TPP)Cl] X-ray structure at 293 K (Figure 2a) can be refined in space group $I4/m$, in full agreement with the previously reported room-temperature structure,[4b] but we found that the crystal structure refinement significantly improves in the space group $I4$ with a decrease in $R1$ value from 0.0620 to 0.0318. At this temperature the porphyrin ring is perpendicular to the c axis within error. The disordered Fe−Cl part above and below the porphyrin plane shows a slight asymmetry in distance from the porphyrin plane (0.33 Å vs 0.49 Å) and occupancy (0.363(1)/0.637(1)), deviating significantly from the 0.5/0.5 ratio imposed by the C_{4h} site symmetry in $I4/m$. At 143 K the mean tilt of the phenyl group plane in $I4$ is 2.8(1)°. The refined residual values in $I4$ are $R1$ = 0.0481 and $wR2$ = 0.1487. The X-ray structure at 20 K was refined against extensive high-resolution synchrotron data, and the agreement indices $R1$, $wR2$ ($I > 2\sigma(I)$), and S are 0.0352, 0.1092, and 1.004, respectively. The site-occupancy ratio for the disordered Fe−Cl part was refined to 0.4084(5)/0.5916(5). The phenyl ring tilt follows the Fe−Cl disorder distribution, and the mean planes of the two disordered phenyl groups are now tilted 6.8(1)° for the major component and 7.7(2)° for the minor component, respectively. As shown in Figure 3, the phenyl rings tilt away from the chloride ligand, a point discussed later.

The neutron structure at 20 K confirms the $I4$ space group symmetry with comparable residual values of $R1$ = 0.0399, $wR2$ = 0.0757, and S = 1.137. The coordinates, equivalent isotropic displacement parameters, and bond lengths and angles for the non-H atoms are within 3 combined standard deviations of those calculated from X-ray diffraction data at 20 K. The observed tilt angle of the phenyl ring away from the c axis is 6.74(9)° and 10.7(3)° for the major and minor components, respectively. The small differences between the X-ray and neutron refinements might be explained by our use of a larger crystal from a different batch for the latter. Figure 3 demonstrates the two configurations of the Fe−Cl part with a slightly asymmetric tilting of the phenyl rings away from the c axis at 20 K, breaking the mirror symmetry in the ab plane.

In comparison to the reported structure of [Fe(TPP)Cl] in $I4/m$ at 100 K,[11] the uneven, ca. 40/60, distribution of the disordered Fe−Cl part on both sides of the porphyrin plane in our structures reveals that the true structure symmetry is $I4$. In addition, the large number of high-resolution data collected at the synchrotron source at 20 K, especially the high-angle data, allow a better determination of the thermal vibrations in comparison to the lower-resolution data using a typical home-source X-ray diffractometer and refines more accurately the occupancy ratio of the disordered Fe−Cl group (vide supra).

Our VT study also revealed the nature of a static disorder of the porphyrin ligand. The out-of-plane phenyl C atoms (C7, C8, C10, and C11) were found disordered in two positions about a common plane parallel to the c axis. The disorder becomes noticable at 143 K and evident at 20 K, as shown in Figure S2c (Supporting Information). Examining the thermal ellipsoid elongation parallel to the mirror plane by the ratio of U_{max}/U_{min} further elucidates the trend of distortion of the refined structure model. The variation of the displacement parameters with temperature is plotted in Figure 4. The ratio in $I4/m$ increases from 2.48 at 293 K to 2.64 at 143 K and doubles to 5.34 at 20 K. However, U_{max}/U_{min} in the refinements in $I4$ increases at a negligible rate (2.53 (293 K), 2.63 (143 K), 2.83 (20 K)) over the same temperature range. This supports the symmetry $I4$ with a static disorder model especially at the low temperature. Alternatively, this trend can be described by the distances between the disordered pairs of carbon atoms C7 and C7′, and C8 and C8′. There is no apparent separation at 293 K, while the distance between C7 and C7′ (as well as C8 and C8′) increases to 0.053 Å at 143 K and further to ca. 0.16 Å at 20 K. The increase in separation distance Δd (Å) with cooling and the "freezing out" of the atomic positions is also displayed in Figure 4. (The disorder behavior of C10 and C11 mirrors that of C7 and C8 and is therefore not described separately.)

dx.doi.org/10.1021/ic5015835 | Inorg. Chem. 2014, 53, 11552−11562

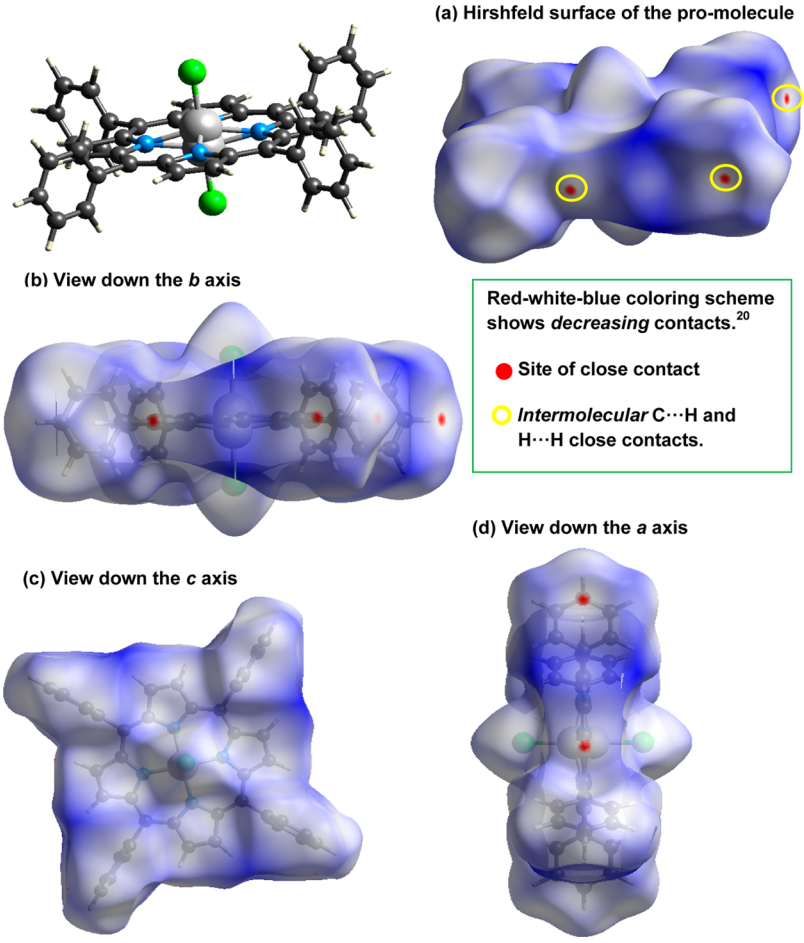

Figure 5. Hirshfeld surface of [Fe(TPP)Cl] showing normalized close distances of the promolecule and neighboring molecules at 293 K. The semitransparent surface shows the enclosed molecule.

The cell volume and parameters decrease as expected from 1800.49(5) Å^3 at 293 K (a = 13.5374(2) Å, c = 9.8247(2) Å) to 1774.5(19) Å^3 at 143 K (a = 13.504(3) Å, c = 9.731(10) Å) and 1760.63(14) Å^3 at 20 K (a = 13.4830(5) Å, c = 9.6849(6) Å). However, the percentage decrease in the c axis (1.4% from 293 to 20 K) is 3 times as large as the percentage decrease in the a axis, as a consequence of the tilting of the phenyl rings, allowing a tighter layer packing along the c axis.

Hirshfeld Surface Analysis of the Crystal Structures of [Fe(TPP)Cl]. The crystal structure analyses above indicate a gradual hardening of the phenyl ring position into two distinct conformations with cooling. Hirshfeld surface analyses of the current and previously reported $I4$[12] and $P2_1/n$ structures[9] have been used to provide further insight.

Hirshfeld surfaces of our crystal structure of [Fe(TPP)Cl] at 293 K are given in Figure 5. Such surfaces at 143 and 20 K are given in Figure S4 (Supporting Information), revealing the development of close-contact sites with temperature. The Hirshfeld volume and surface area of our 293 K structure, 888.55 Å^3 and 677.40 Å^2, respectively, are very similar to 893.18 Å^3 and 677.52 Å^2 for the reported $I4$ structure at 293 K.[12] The reported monoclinic $P2_1/n$ structure,[9a] used as a baseline comparison here, is more compact with a significantly smaller Hirshfeld volume and surface area: 840.26 Å^3 and 655.38 Å^2, respectively.[9a] The fingerprint plots for our room-temperature $I4$ and the monoclinic $P2_1/n$ structures in Figure 6a,b (H···H close contacts) and Figure 6c,d (Cl···H close contacts) reveal distinctly different shapes, reflecting the molecular stacking of parallel layers for the former and a herringbone arrangement for the latter. The Cl···H contacts are further apart in the monoclinic structure and contribute significantly less to the Hirshfeld surface in comparison to those in the tetragonal structure (Figure S6, Supporting Information). A less-strained monoclinic structure is favored by larger axial Br^- and I^- ligands ([Fe(TPP)Br] in $P2_1/c$;[37] [Fe(TPP)I] in $P2_1/n$[38]). Tetragonal structures predominate for smaller halides F^- (in [Fe(TPP)F][39]) and Cl^-.

It has been reported that the phenyl rings tilt in the structure of [Co(TPP)Cl] as a result of intermolecular interactions.[40] We have investigated how phenyl rings tilt in the iron analogue [Fe(TPP)Cl] and separated two phenyl tilt options,[41] toward or away from the Cl ligand, in our 20 K X-ray structure to give two Hirshfeld fingerprint plots, emphasizing close intermolecular Cl···H contacts (Figure 7). The plots show two significantly different contacts: (a) 2.7018 Å (Figure 7a) with a void volume of 336.24 Å^3 when the phenyl rings tilt *toward* the chloride; (b) 3.966 Å (Figure 7b) with a void volume of 325.51 Å^3 when the phenyl rings tilt *away* from the chloride. The larger void volume in (a) accompanies the shorter contact of 2.7018 Å. This distance is smaller than the sum of the van der Waals radii of H (1.20 Å) and Cl (1.75 Å) atoms,[42] and the close proximity prohibits further tilting and compression. The opposite tilting in (b) provides a comfortable distance and has room for further tilt. Both considerations make the

dx.doi.org/10.1021/ic5015835 | Inorg. Chem. 2014, 53, 11552−11562

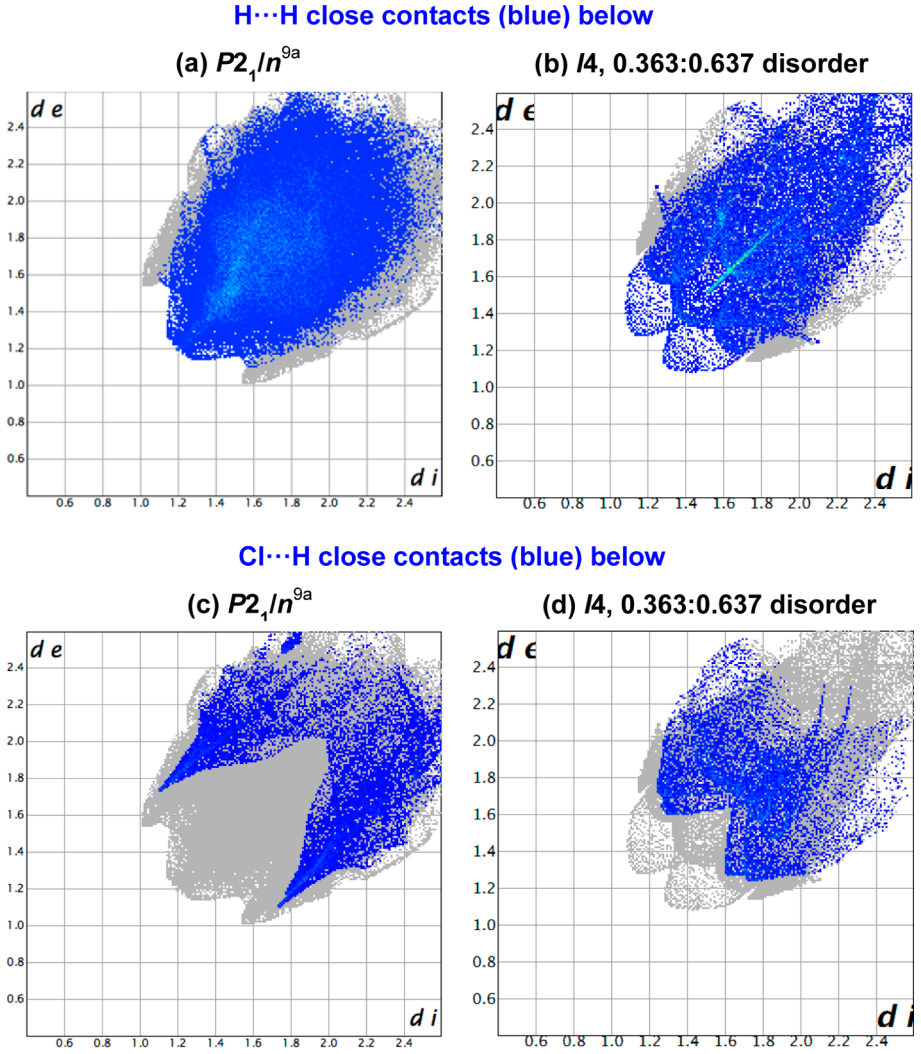

Figure 6. Hirshfeld fingerprint plots for the [Fe(TPP)Cl] structures at 293 K in $P2_1/n$[9a] and $I4$ from the current work. The closest contacts correspond to the minimum values of $d_e + d_i$ in each plot: e.g., 2.8 Å for Cl···H in (c) and 2.9 Å for Cl···H in (d).

configuration in (a) unlikely and favor (b), where the Cl and H atoms are further away from each other.

Hirshfeld Surface Analysis of the Crystal Structure of [Co(TPP)(NO)]. VT studies have been published on crystal structures of [Fe(TPP)(NO)] and [Co(TPP)(NO)],[11,13g,18] focusing on the structural disorder of the NO ligand at room temperature and gradual ordering of the NO ligand with cooling, resulting in a phase change with symmetry lowering from $I4/m$ to $P\bar{1}$.[11,13g] The Hirshfeld surface area and volume for [Co(TPP)(NO)] change little and contract only 1.3% and 2.5%, respectively, with decreasing temperature, despite the phase change and the reduction in the disorder of the nitrosyl ligand (Table 2). Close to the phase transition at 195 K significant intermolecular contacts between the nitrosyl oxygen and the hydrogen atoms on the phenyl rings of the adjacent molecules are noticable (Figure 8a, red spots). After the phase transition (Figure 8b), a decrease in these close intermolecular contacts is immediate and obvious. In the tetragonal $I4/m$ phase, the NO ligand is disordered in four positions above and four positions below the porphyrin plane, a total of 8-fold disorder. The disorder is taken into account for the Hirshfeld surface calculations according to McKinnon et al.[22] The nearest O···H contacts (~2.5 Å) in $P\bar{1}$ are farther away than the contacts (~2.3 Å) in $I4/m$ (Figure 9). This decrease in intermolecular contacts can be explained by the tilting of the phenyl rings, which in effect traps the disordered NO ligand. By 180 K, the disordered NO ligand is trapped into a single position above and below the porphyrin plane, which are related to each other by an inversion center. This phase change in [Co(TPP)(NO)] is abrupt, immediately increasing both the Hirshfeld surface and void volume by more than 1%. The void-volume percentage in the cell increases from 15.42% at 195 K before to 16.47% at 190 K after the phase transition (Table 2 and Figure 10).

A contraction of the crystal lattice is expected with cooling. This is apparent in the relative contributions of the close intermolecular contacts to the Hirshfeld surface (Figure 11). The percent H···H and C···H close contacts gradually increase with decreasing temperature. Interestingly, after the phase change, the percent O···H contacts are reduced while the N···H close contacts are increased significantly, signifying the ordering of the nitrosyl ligand with the phenyl tilt. The closest N···H close contacts are 2.957 Å before the phase change and 2.696 Å after the phase change (Figure S9, Supporting Information).

Hirshfeld Surface Analysis of the Crystal Structure of [Fe(TPP)(NO)]. The crystal structures of [Fe(TPP)(NO)][13g] and [Co(TPP)(NO)][11] are isomorphous. Unlike [Co(TPP)(NO)] with a clear phase change at 190–195 K,[11] the change

dx.doi.org/10.1021/ic5015835 | Inorg. Chem. 2014, 53, 11552–11562

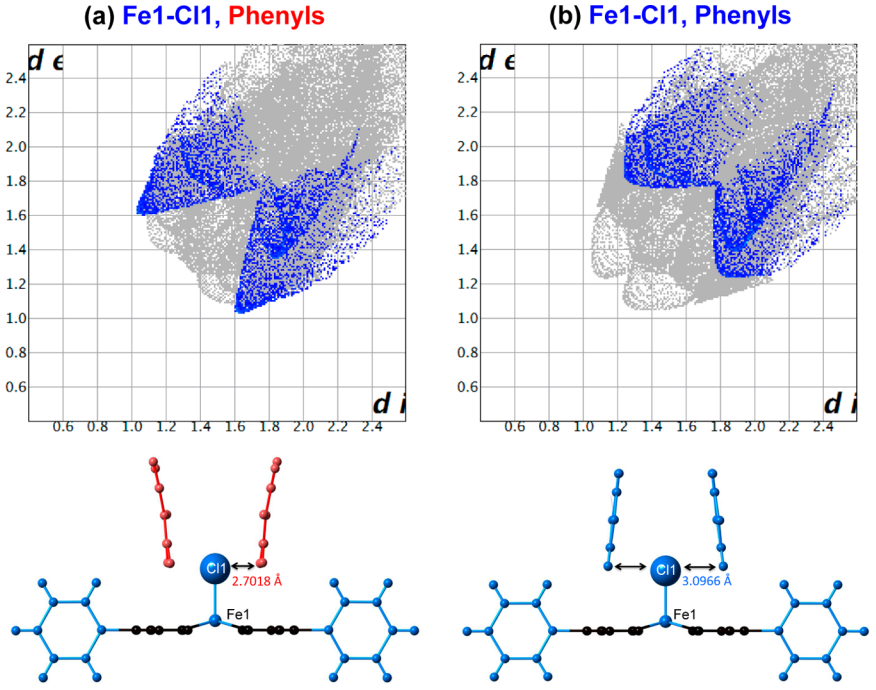

Figure 7. Hirshfeld fingerprints of Cl···H close contacts in the X-ray [Fe(TPP)Cl] structure at 20 K in *I*4 with parts of Figure 3 reproduced, indicating that the configuration in (b) is preferred.[41]

Table 2. Comparison of the Hirshfeld Surfaces and Void Volumes

complex	temp (K)	space group	Hirshfeld volume (Å^3)	Hirshfeld area (Å^2)	void volume in the cell volume (%)
[Fe(TPP)Cl]	293	*I*4	888.55	677.40	17.21
	143	*I*4	875.55	674.85	16.42
	100[11]	*I*4/*m*	865.71	668.79	15.84
	20	*I*4	868.02	674.29	10.19
[Co(TPP)(NO)][11]	250	*I*4/*m*	854.01	663.56	15.27
	195	*I*4/*m*	859.31	667.66	15.42
	190	$P\bar{1}$	868.55	671.18	16.47
	180	$P\bar{1}$	855.31	664.72	16.20
	100	$P\bar{1}$	833.01	655.22	14.71
[Fe(TPP)(NO)][13g]	293	*I*4/*m*	875.44	675.08	16.16
	180	$P\bar{1}$	860.04	668.09	16.00
	90	$P\bar{1}$	849.32	664.76	15.14
	33	$P\bar{1}$	845.26	663.53	14.79

in [Fe(TPP)(NO)] is gradual.[13g] Hirshfeld fingerprint plots showing the intermolecular close contacts are given in Figure S10 (Supporting Information). The Hirshfeld surface area and volume for [Fe(TPP)(NO)] only slightly contract, by 1.7% and 3.4% respectively, with cooling. At 293 K, the 4-fold disorder of the NO lignand leads to very close contacts with four adjacent phenyls (red areas in Figure 8c). The tilted four phenyl groups surrounding the NO ligand below the phase change at 33 K are shown in Figure 12. The top is a view along the *c* axis with all four rings, and the left shows the phenyl rings A and B parallel to the nitrosyl ligand. The closest H atoms on the A and B phenyl rings are equal in distance (2.8130 and 2.8133 Å, respectively) to the O atom on the nitrosyl ligand. However, the N atom of the nitrosyl ligand is much closer to the H atom on B (2.5609 Å) than to the H atom on A (3.4074 Å). The structure on the right shows the phenyl rings C and D, perpendicular to the nitrosyl bond. The tilting of D toward the nitrosyl leads to a short distance (2.6411 Å) of its nearest H atom to the O atom and a fairly long distance (3.3095 Å) to the N atom. In C, the opposite is true: the nearest H atom is much closer to the N atom (2.6874 Å) than to the O atom (3.1594 Å).

Comparison of the Hirshfeld Surface Analyses of [M(TPP)X] (M = Fe, X = Cl; M = Co, Fe, X = NO). After the phase changes for both nitrosyl complexes, the Hirshfeld surface areas and volumes as well as the percentage of the void volume in the unit cell are similar (Table 2, 180 K). Like [Fe(TPP)Cl], [Fe(TPP)(NO)] exhibits a similar structural softness through a gradual adjustment of the structure with temperature, making it difficult to determine the crystal structure over an extended temperature range. In contrast to [Co(TPP)(NO)], the characteristic increase of the Hirshfeld volume or void-volume percentage after the phase change from *I*4/*m* to $P\bar{1}$ in [Fe(TPP)(NO)] could not be observed. The Fe(III) ion is slightly larger than the Co(III) ion.[43] As a result, the Fe−ligand bonds in [Fe(TPP)(NO)] are less ionic than those in [Co(TPP)(NO)], perhaps leading to the structural softness in the former.

dx.doi.org/10.1021/ic5015835 | *Inorg. Chem.* 2014, 53, 11552−11562

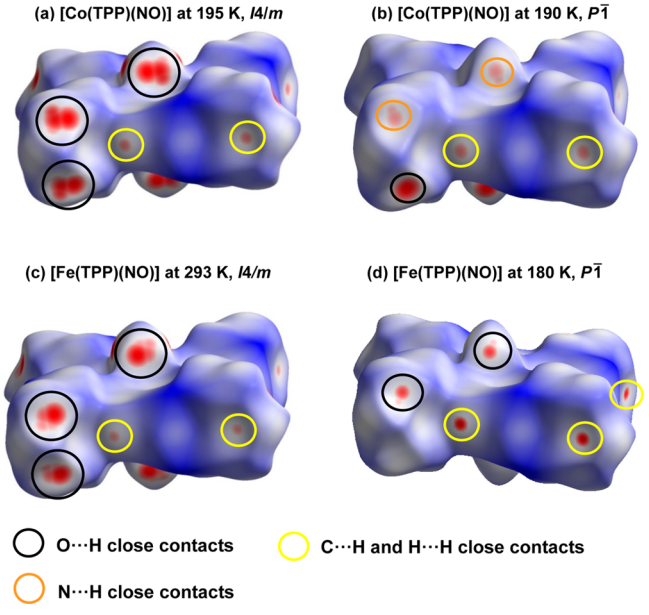

Figure 8. Hirshfeld surfaces for the crystal structures of [Co(TPP)(NO)] and [Fe(TPP)(NO)] before and after the phase changes.

More importantly, the phase change in both nitrosyl complexes involves phenyl tilting as in [Fe(TPP)Cl]. Independent of the symmetric (Cl) or asymmetric (NO) apical ligand, the tilting is associated with cooling and plays a noticeable role in the ability of these metalloporphyrins to structurally compress. In the previous, traditional structural analysis (without considering the Hirshfeld surface analysis), in comparison, the phenyl contribution to the phase change is overshadowed by the disorder in the asymmetric NO ligands.

■ CONCLUDING REMARKS

Metalloporphyrins have been studied intensely for decades. The basic structural analyses, typically focused on bond distances and angles, do not show significant changes in these parameters with cooling or phase changes. Such analyses, however, hardly reveal "available space" found in voids that become important to explain options for structural compression and phase changes. Furthermore, it has proved difficult to use the structural analyses when significant symmetry changes accompany phase changes. Hirshfeld analysis is employed in the current work to showcase how conformational changes appear in the molecular structures and to identify driving forces for such changes that are otherwise not obvious as a result of disorder or twinning.

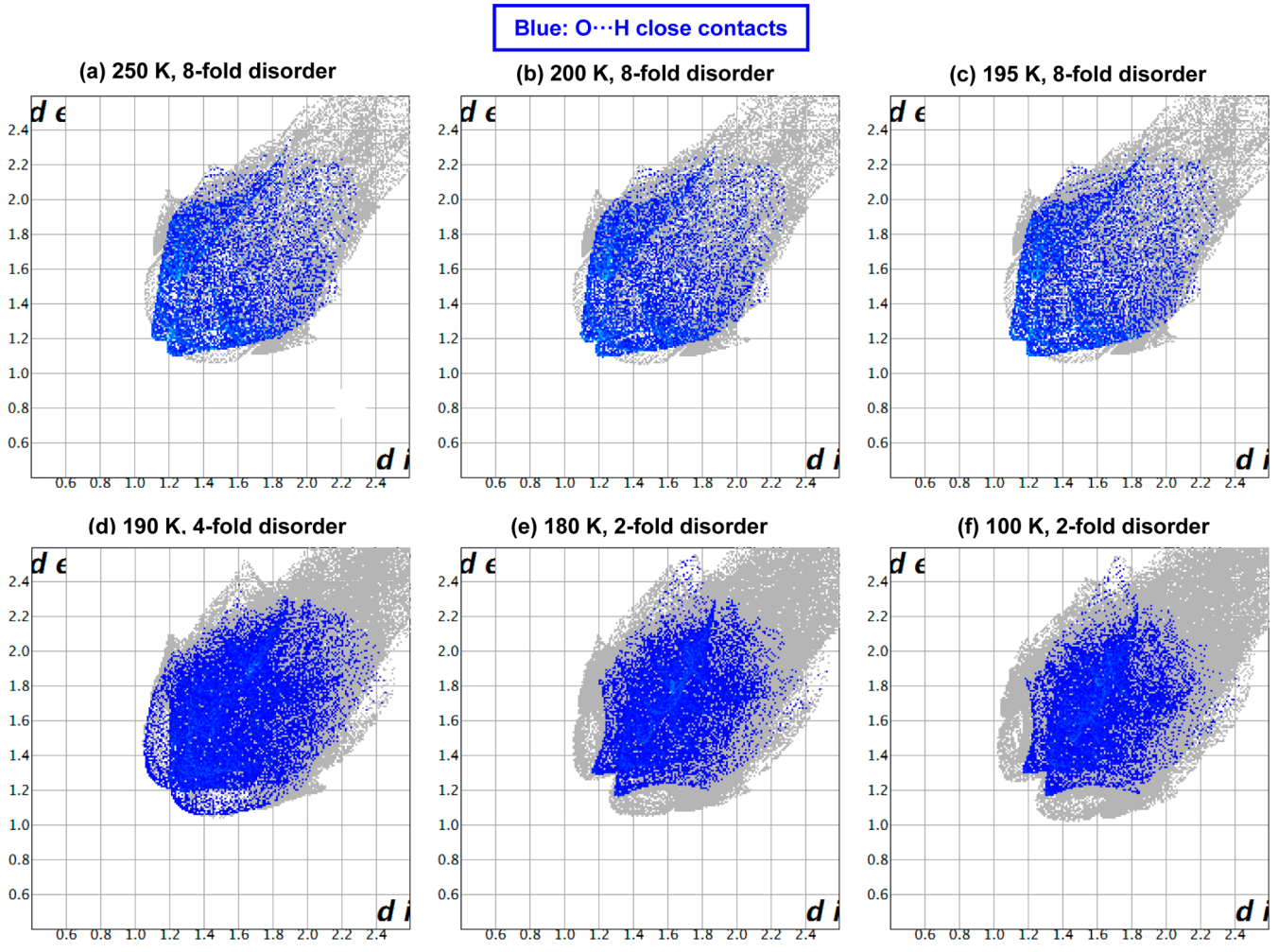

Figure 9. Hirshfeld fingerprint plots of [Co(TPP)(NO)] (O···H close contacts).

dx.doi.org/10.1021/ic5015835 | Inorg. Chem. 2014, 53, 11552−11562

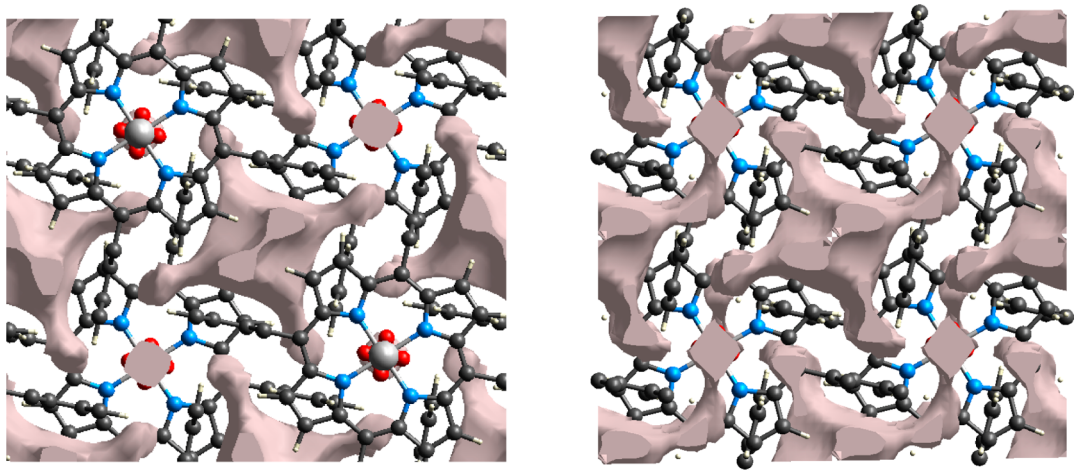

Figure 10. Voids of [Co(TPP)(NO)] at 195 K (left, $I4/m$) and 190 K (right, $P\bar{1}$) using an isovalue of 0.002 e au^{-3}.

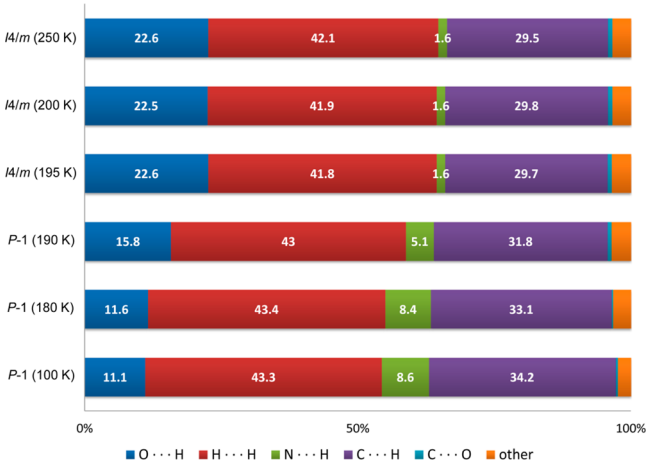

Figure 11. Percentage contributions to the Hirshfeld surface area for various intermolecular close contacts for [Co(TPP)(NO)] molecules.

Studies here illustrate the temperature-dependent structural characteristics to help understand the intricate interplay of structural and conformational flexibility of the metalloporphyrins, revealing that the disorders in the crystal structures of [Fe(TPP)(NO)] and [Co(TPP)(NO)] at room temperature and phase changes at lower temperatures are a result of intermolecular interactions in the solid state. The phase changes in [Fe(TPP)(NO)] and [Co(TPP)(NO)], accompanied by the phenyl tilting, lead to reduced intermolecular interactions by gradual movement of the phenyl groups into the open voids. The same occurs in [Fe(TPP)Cl] with no phase change.

Hirshfeld surface analyses as a whole-of-molecule approach allow for an objective way to compare crystal structures of different crystal symmetries but with similar molecular forces and interactions. The phase change appears to be as much driven by phenyl tilting away from the c axis into the void space as by the ordering of the nitrosyl ligand. It is the void volume, not the increase in the individual molecular density, that accommodates further thermal compression with cooling. The analyses of the three compounds suggest that other metalloporphyrins with the general formula [M(TPP)X] in the tetragonal system may show analogous behavior of the phenyl rings contributing considerably to phase changes at low temperatures.

■ ASSOCIATED CONTENT

Supporting Information

Text, figures, tables, and CIF files giving additional experimental details, a photograph of the crystal used in the neutron diffraction study, a diagram overlapping the X-ray crystal structures refined in $I4/m$ and $I4$, a packing plot of the [Fe(TPP)Cl] crystal structure at 293 K, additional Hirshfeld surfaces and fingerprint plots of [Fe(TPP)Cl], [Co(TPP)(NO)], and [Fe(TPP)(NO)], refinement data in $I4/m$ and $I/4$ for the structure of [Fe(TPP)Cl], its atomic coordinates, isotropic displacement parameters, bond lengths and angles, and hydrogen bonding from 20 K neutron data. This material is available free of charge via the Internet at http://pubs.acs.org.

■ AUTHOR INFORMATION

Corresponding Authors

*Email for C.M.H.: choffmann@ornl.gov.
*E-mail for X.W.: wangx@ornl.gov.
*E-mail for Z.-L.X.: xue@utk.edu.

Present Address

[⊥]The Bragg Institute, Australian Nuclear Science and Technology Organisation, Lucas Heights, NSW 2234, Australia.

Notes

The authors declare no competing financial interest.

■ ACKNOWLEDGMENTS

We thank the Joint Institute for Neutron Sciences (JINS) fellowship program (S.C.H. and B.A.S.) and the U.S. National Science Foundation (CHE-0516928, CHE-1012173, and CHE-1362548 to Z.X.) for funding, ANL's Advanced Photon Source on beamline 15ID-C for X-ray data at 20 K, and the Institut Laue-Langevin for the allocation of neutron beam time on D9. Acknowledgment is also made to the donors of the American Chemical Society Petroleum Research Fund for partial support of this research. Beamline 15ID-C is principally supported by the National Science Foundation/Department of Energy under Grant CHE-1346572. ANL is a U.S. Department of Energy laboratory operated by The University of Chicago at Argonne, LLC, under Contract DE-AC02-06CH11357. ORNL/SNS is managed by UT-Battelle, LLC, for the U.S. Department of Energy under contract DE-AC05-00OR22725.

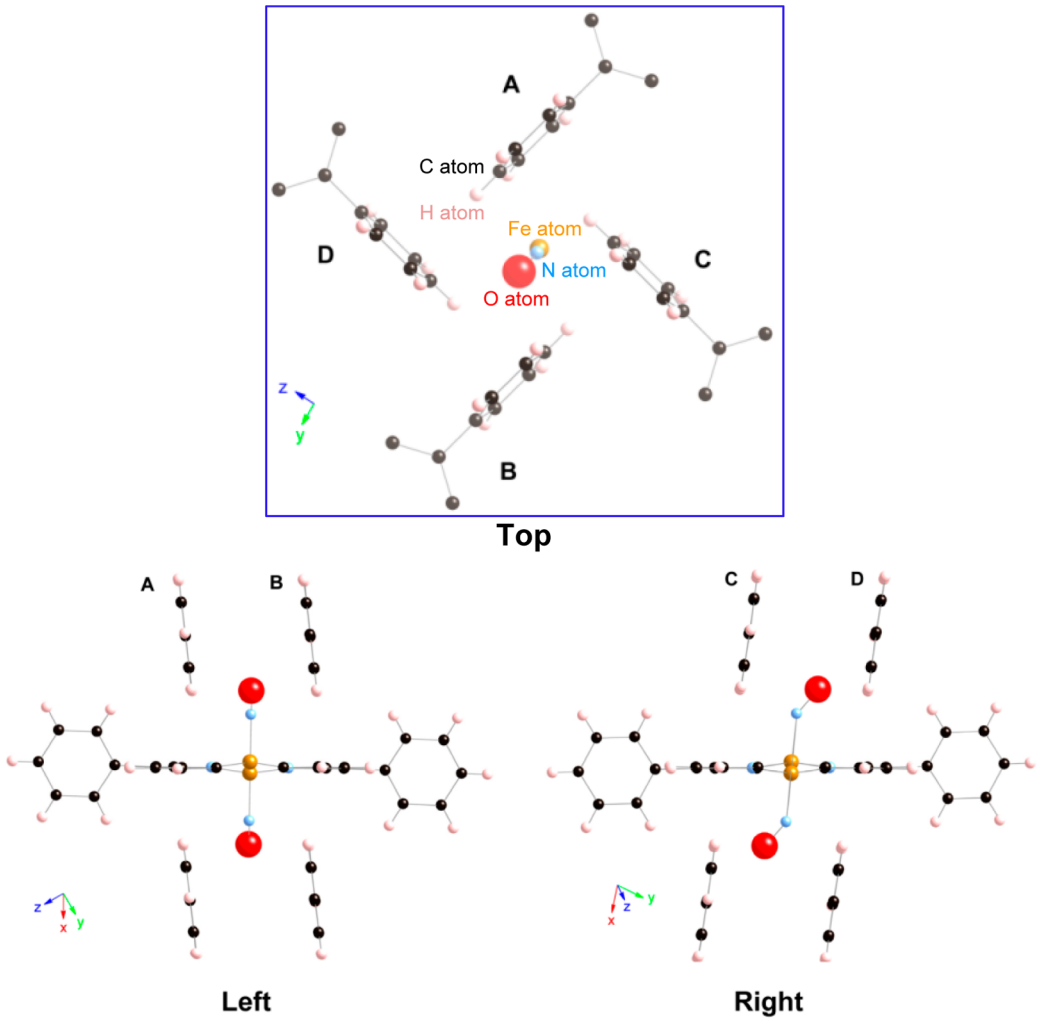

Figure 12. Phenyl ring tilt in [Fe(TPP)(NO)] at 33 K: (top) phenyl rings surrounding a NO ligand; (bottom left) tilting of the phenyl rings A and B which are parallel to the nitrosyl bond (phenyl rings C and D and other atoms are omitted for clarity); (bottom right) tilting of the phenyl rings C and D which are perpendicular to the nitrosyl bond (phenyl rings A and B and other atoms are omitted for clarity).

REFERENCES

(1) Behere, D. V.; Birdy, R.; Mitra, S. *Inorg. Chem.* **1982**, *21*, 386.

(2) D'Angelo, P.; Lapi, A.; Migliorati, V.; Arcovito, A.; Benfatto, M.; Roscioni, O. M.; Meyer-Klaucke, W.; Della-Longa, S. *Inorg. Chem.* **2008**, *47*, 9905.

(3) Scheidt, W. R.; Gouterman, M. In *Iron Porphyrins*; Lever, A. B. P., Gray, H. B., Eds.; Addison-Wesley: Reading, MA, 1983; Part One, pp 89−139.

(4) (a) Fleischer, E. B.; Miller, C. K.; Webb, L. E. *J. Am. Chem. Soc.* **1964**, *86*, 2342. (b) Hoard, J. L.; Cohen, G. H.; Glick, M. D. *J. Am. Chem. Soc.* **1967**, *89*, 1992.

(5) Eaton, D. R.; LaLancette, E. A. *J. Chem. Phys.* **1964**, *41*, 3534.

(6) Collman, J. P.; Hoard, J. L.; Kim, N.; Lang, G.; Reed, C. A. *J. Am. Chem. Soc.* **1975**, *97*, 2676.

(7) Cheng, R. J.; Chen, P. Y.; Lovell, T.; Liu, T.; Noodleman, L.; Case, D. A. *J. Am. Chem. Soc.* **2003**, *125*, 6774.

(8) Mao, J.; Zhang, Y.; Oldfield, E. *J. Am. Chem. Soc.* **2002**, *124*, 13911.

(9) (a) Scheidt, W. R.; Finnegan, M. G. *Acta Crystallogr., Sect. C.* **1989**, *C45*, 1214. The CIF file was obtained from the Cambridge Crystallographic Data Centre using the DOI of the paper: doi: 10.1107/S0108270189000715. (b) Finnegan, M. G.; Lappin, A. G.; Scheidt, W. R. *Inorg. Chem.* **1990**, *29*, 181.

(10) Hunter, S. C.; Podlesnyak, A. A.; Xue, Z. L. *Inorg. Chem.* **2014**, *53*, 1955.

(11) Grande, L. M.; Noll, B. C.; Oliver, A. G.; Scheidt, W. R. *Inorg. Chem.* **2010**, *49*, 6552.

(12) Corban, G. J.; Hadjikakou, S. K.; Tsipis, A. C.; Kubicki, M.; Bakas, T.; Hadjiliadis, N. *New J. Chem.* **2011**, *35*, 213 The CIF file deposited in the Cambridge Crystallographic Data Centre (CCDC No. 783326) was used..

(13) (a) Moncada, S.; Palmer, R. M.; Higgs, E. A. *Pharmacol. Rev.* **1991**, *43*, 109. (b) Ignarro, L.: *Nitric Oxide: Biology and Pathobiology*; Academic Press: San Diego, CA, 2000. (c) Lehnert, N.; Berto, T. C.; Galinato, M. G. I.; Goodrich, L. E. The Role of Heme-Nitrosyls in the Biosynthesis, Transport, Sensing, and Detoxification of Nitric Oxide (NO) in Biological Systems: Enzymes and Model Complexes. In *The Handbook of Porphyrin Science*; Kadish, K. M., Smith, K. M., Guilard, R., Eds.; World Scientific: Hackensack, NJ, 2011; Vol. *14*, Chapter 63, pp 1−247. (d) Goodrich, L. E.; Paulat, F.; Praneeth, V. K. K.; Lehnert, N. *Inorg. Chem.* **2010**, *49*, 6293. (e) Straub, A. C.; Lohman, A. W.; Billaud, M.; Johnstone, S. R.; Dwyer, S. T.; Lee, M. Y.; Bortz, P. S.; Best, A. K.; Columbus, L.; Gaston, B.; Isakson, B. E. *Nature* **2012**, *491*, 473. (f) Gladwin, M. T.; Kim-Shapiro, D. B. *Nature* **2012**, *491*, 344. (g) Silvernail, N. J.; Olmstead, M. M.; Noll, B. C.; Scheidt, W. R. *Inorg. Chem.* **2009**, *48*, 971. (h) Zheng, H. W.; Wang, R. B.; Qiao, L. K.; Du, Y. *Sci. China Technol. Sci.* **2014**, *57*, 857.

(14) (a) Wang, H.; Zhong, F.; Pan, J.; Li, W.; Su, J.; Huang, Z.-X.; Tan, X. *J. Biolog. Inorg. Chem.* **2012**, *17*, 719. (b) Garthwaite, J. *Trends Neurosci.* **1991**, *14*, 60.

(15) (a) Fritz, B. G.; Roberts, S. A.; Ahmed, A.; Breci, L.; Li, W.; Weichsel, A.; Brailey, J. L.; Wysocki, V. H.; Tama, F.; Montfort, W. R. *Biochemistry* **2013**, *52*, 156. (b) Rapoport, R. M.; Murad, F. *Circ. Res.* **1983**, *52*, 352. (c) Ignarro, L. J.; Adams, J. B.; Horwitz, P. M.; Wood, K. S. *J. Biol. Chem.* **1986**, *261*, 4997.
(16) (a) Azuma, H.; Ishikawa, M.; Sekizaki, S. *Br. J. Pharmacol.* **1986**, *88*, 411. (b) Furlong, B.; Henderson, A. H.; Lewis, M. J.; Smith, J. A. *Br. J. Pharmacol.* **1987**, *90*, 687.
(17) (a) Campbell, M. G.; Underbakke, E. S.; Potter, C. S.; Carragher, B.; Marletta, M. A. *Proc. Natl. Acad. Sci. U.S.A.* **2014**, *111*, 2960. (b) Ursu, O. N.; Sauter, M.; Ettischer, N.; Kandolf, R.; Klingel, K. *Cell. Physiol. Biochem.* **2014**, *33*, 52.
(18) (a) Scheidt, W. R.; Frisse, M. E. *J. Am. Chem. Soc.* **1975**, *97*, 17. (b) Scheidt, W. R.; Hoard, J. L. *J. Am. Chem. Soc.* **1973**, *95*, 8281.
(19) (a) Scheidt, W. R.; Barabanschikov, A.; Pavlik, J. W.; Silvernail, N. J.; Sage, J. T. *Inorg. Chem.* **2010**, *49*, 6240. (b) Kim, H.; Chang, Y. H.; Lee, S.-H.; Lim, S.; Noh, S.-K.; Kim, Y.-H.; Kahng, S.-J. *Chem. Sci.* **2014**, *5*, 2224. (c) Sulok, C. D.; Bauer, J. L.; Speelman, A. L.; Weber, B.; Lehnert, N. *Inorg. Chim. Acta* **2012**, *380*, 148. (d) Lehnert, N.; Galinato, M. G. I.; Paulat, F.; Richter-Addo, G. B.; Sturhahn, W.; Xu, N.; Zhao, J. Y. *Inorg. Chem.* **2010**, *49*, 4133.
(20) Spackman, M. A.; Jayatilaka, D. *CrystEngComm* **2009**, *11*, 19.
(21) Spackman, M. A.; McKinnon, J. J. *CrystEngComm* **2002**, *4*, 378.
(22) McKinnon, J. J.; Jayatilaka, D.; Spackman, M. A. *Chem. Commun.* **2007**, 3814.
(23) Turner, M. J.; McKinnon, J. J.; Jayatilaka, D.; Spackman, M. A. *CrystEngComm* **2011**, *13*, 1804.
(24) Dougan, B. A. Ph.D. Dissertation, The University of Tennessee, Knoxville, TN, 2009.
(25) Poulsen, R.; Bentien, A.; Graber, T.; Iverson, B. *Acta Crystallogr., Sect. A* **2004**, *A60*, 382.
(26) *SAINT-PLUS, Version 6.02 (including XPREP)*; Bruker AXS Inc., Madison, WI, USA, 2003.
(27) *APEX2. Version 2.14*; Bruker AXS Inc., Madison, WI, USA, 2007.
(28) Sheldrick, G. M. *SADABS*; University of Göttingen, Göttingen, Germany, 2003.
(29) Lehmann, M. S.; Kuhs, W.; Allibon, J.; Wilkinson, C.; McIntyre, G. J. *J. Appl. Crystallogr.* **1989**, *22*, 562.
(30) Wilkinson, C.; Khamis, H. W.; Stansfield, R. F. D.; McIntyre, G. J. *J. Appl. Crystallogr.* **1988**, *21*, 471.
(31) Coppens, P.; Leiserowitz, L.; Rabinovich, D. *Acta Crystallogr.* **1965**, *18*, 1035.
(32) Howard, J. A. K.; Johnson, O.; Schultz, A. J.; Stringer, A. M. *J. Appl. Crystallogr.* **1987**, *20*, 120.
(33) Sheldrick, G. M. *Acta Crystallogr., Sect. A* **2008**, *A64*, 112.
(34) Spek, A. L. *J. Appl. Crystallogr.* **2003**, *36*, 7.
(35) Wolff, S. K.; Grimwood, D. J.; McKinnon, J. J.; Turner, M. J.; Jayatilaka, D.; Spackman, M. A. *CrystalExplorer (Version 3.1)*; University of Western Australia, 2012.
(36) (a) Sakurai, T.; Yamamoto, K.; Naito, H.; Nakamoto, N. *Bull. Chem. Soc. Jpn.* **1976**, *49*, 3042. (b) Coutsolelos, A.; Guilard, R.; Bayeul, D.; Lecomte, C. *Polyhedron* **1986**, *5*, 1157. (c) Cheng, B.; Scheidt, W. R. *Acta Crystallogr., Sect. C* **1996**, *C52*, 361.
(37) Skelton, B. W.; White, A. H. *Aust. J. Chem.* **1971**, *30*, 2655.
(38) Hatano, K.; Scheidt, W. R. *Inorg. Chem.* **1979**, *18*, 877.
(39) Anzai, K.; Hatano, K.; Lee, Y. J.; Scheidt, W. R. *Inorg. Chem.* **1981**, *20*, 2337.
(40) Sakurai, T.; Yamamoto, K. *Sci. Paper. Inst. Phys. Chem. Res.* **1976**, *70*, 31.
(41) Two CIF files were generated with the following ratios of Fe−Cl part/phenyls: 0.4084/0.5916 (Figure 7a), 0.4084/0.4084 (Figure 7b). These CIF files were used to generate the fingerprints in Figure 7a,b.
(42) Rowland, R. S.; Taylor, R. *J. Phys. Chem.* **1996**, *100*, 7384.
(43) Shannon, R. D. *Acta Crystallogr., Sect. A* **1976**, *A32*, 751.